

## **Optical and Photocurrent Spectroscopy Studies of Inter- and Intra-Band Transitions in Size-Tailored InAs/GaAs Quantum Dots**

I. MUKHAMETZHANOV, Z. H. CHEN, O. BAKLENOV, E. T. KIM, and A. MADHUKAR<sup>1)</sup>

*Departments of Materials Science and Physics, University of Southern California, 3651 Watt Way, VHE 506, Los Angeles, CA 90089-0241, USA*

(Received July 31, 2000; accepted October 2, 2000)

Subject classification: 68.65.Hb; 73.21.La; 73.63.Kv; 78.55.Cr; S7.12

Combined inter- and intra-band spectroscopy studies are presented on structurally well-characterized InAs/GaAs(001) self-assembled quantum dots grown via conventional continuous deposition and the innovative punctuated island growth approach. Temperature and power dependent photoluminescence (PL) and PL Excitation (PLE) on these remarkably uniform quantum dot based samples (with typical PL linewidth  $\approx 25$  meV), reveal details of size-dependent electronic structure. These studies are complemented with systematic near- and middle-infrared photocurrent spectroscopy for inter-band through electron intra-band transitions as a function of temperature and applied electric field.

Epitaxial 3D island quantum dots (QDs) have been a subject of extensive research for the last decade, governed by interest in the physics of 0D systems and their potential for semiconductor devices [1]. However, due to the stochastic nature of such QD formation, the ensemble of QDs does not fully realize its potential due to difficulty in control of QD average size and uniformity. Thus control of these parameters through innovations in deposition conditions and growth procedure becomes crucial for investigation and applications of QDs.

The materials system used for systematic studies of QD photoresponse is the binary InAs/GaAs(001). QD capping is done using migration enhanced epitaxy (MEE) at low temperatures between 350 and 400 °C to minimally impact the QD shape and to reduce intermixing during capping. This allows reasonable comparison between the photoresponse and the structural parameters obtained through AFM and TEM work on identically grown but uncapped QD samples. We have reported that MEE capping at these low temperatures not only preserves the quality of GaAs cap, but also increases the PL efficiency compared to samples grown identically but capped via standard MBE growth techniques [2]. For all growths, GaAs(001)  $\pm 0.1^\circ$  substrates are used and after standard preparation procedures, a GaAs buffer  $\approx 0.5 \mu\text{m}$  thick is grown at 600 °C at rate 0.5 ML/s with short term ( $\approx 2$  min) surface annealing at 613 °C before reducing the substrate temperature to 500 °C for InAs deposition. Various deposition amounts of InAs are delivered at 0.22 ML/s using two growth approaches. After InAs deposition, the substrate temperature is ramped down in  $\approx 1$  min to the capping temperature of 400 or 350 °C, followed by 170 ML MEE GaAs capping at 0.25 ML/s for optical samples, or down to room temperature for uncapped counterparts intended for AFM studies.

---

<sup>1)</sup> Corresponding author; Tel.: +1-213-740-4325; Fax: +1-213-740-4333; e-mail: madhukar@almaak.usc.edu

Figure 1 illustrates the range of size control realizable in single layer QD samples through use of two growth approaches: the usual continuous [3] and the novel punctuated growth [4]. Punctuated island growth approach (PIG) divides the total deposited material into two or more stages, with the first stage being in the well formed island regime, i.e. above critical deposition amount for QD formation. The importance of the punctuation stage is to keep the island density high, since the technique of sub-ML incremental deposition [5] gives generally much lower QD densities compared to continuous deposition case. Interruption gives time for material to redistribute, so that during resumed deposition the probability of new island formation is suppressed. Uniformity comes from the slower growth rate of larger islands due to strain build-up at the island base edge, thus giving smaller islands the opportunity to reach the size-range of the larger ones and reduce nonuniformity [4]. In fact, AFM size analysis shows that virtually all islands have about the same base size ( $\approx 21$  nm diameter, assuming cone-shaped islands), while the heights vary significantly from  $\approx 3.5$  nm, the most probable value for QDs with PL peak at  $\approx 1.18$  eV, to  $\approx 8.5$  nm for QDs with peak at 1.07 eV, as shown in Fig. 1. The corresponding aspect ratio (height to base diameter) changes from  $\approx 0.16$  for small QDs to  $\approx 0.4$  for large QDs. An aspect ratio of 0.16 may be attributed to a variety of sidefacets  $\{203\}$ ,  $\{113\}$ ,  $\{136\}$ , etc. cited in the literature for small QDs, while 0.4 is suggestive of  $\{101\}$  type sidefacets for large islands. TEM on uncapped QD samples confirms AFM findings and reveals QD cross-section in the  $[110]$  azimuth for large islands to be triangular with base size  $\approx 21$  nm and slope  $\approx 36^\circ$ . This slope is consistent with  $\{101\}$  facets. These QDs may actually have multifacet structure analogous to Ge/Si QDs [6], but the available resolution in AFM and TEM does not allow to clarify this issue. QD profile imaging done on the same island using  $[110]$ ,  $[100]$ , and  $[1\bar{1}0]$  azimuths in TEM shows similar shape and size, thus suggesting a quite symmetric QD geometry without significant preferred elongation in these islands.

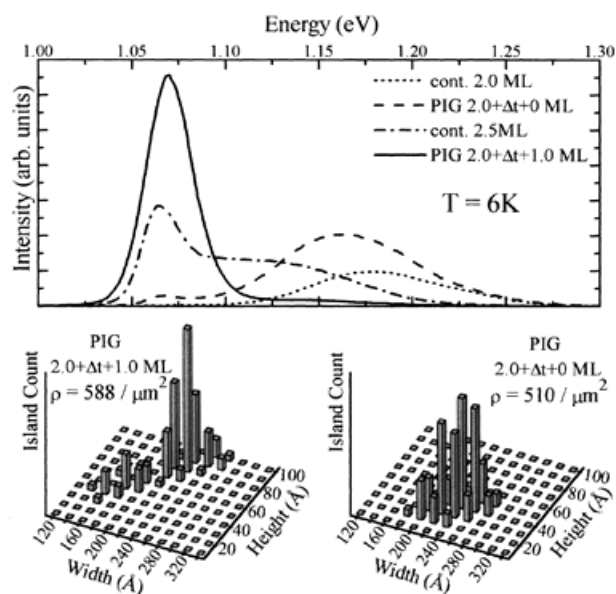


Fig. 1. Low temperature photoluminescence of four typical samples grown via continuous and punctuated (PIG) approaches. Lower panels depict AFM size distribution for two of these to emphasize similarity in lateral size but significant change in height as the island grows

The self-limiting base-size in such islands leads to dramatically reduced PL linewidths (typically  $\approx 25$  meV for large PIG QDs), and to remarkable reproducibility of QD growth, which has allowed us to study their electronic structure using photoluminescence/photoluminescence excitation (PL/PLE) optical spectroscopy and near- and middle-infrared photocurrent (PC) spectroscopy. Figure 2 shows typical high density PL and ground state PLE spectra. High density PL due to inhomogeneous broadening reveals only the strongest optical transition while PLE from the subensemble of QDs defined by the choice of detection wavelength reveals a variety of transitions, the strongest being at  $\approx 89$  and  $\approx 171$  meV above the ground state transition, and weaker transitions at  $\approx 62$  and  $\approx 131$  meV. Oscillator strength of transitions and a qualitative comparison with recent electronic structure calculations on QDs with similar size and shape [7] allow to extract the lowest electronic levels, the electron states being  $\approx 62$  and  $\approx 104$  meV above the electron ground state, and the hole states being  $\approx 27$  and  $\approx 67$  meV above the hole ground state. Resolution of further higher states is low due to their much higher sensitivity to the QD size and shape fluctuations even within the subensemble defined by the chosen detection energy. Multipeak fit to PLE spectra suggests a much richer variety of possible levels and transitions. Thus, the cited levels represent the electronic structure with the strongest optical response. With varying detection wavelength through the inhomogeneously broadened ground state PL, we probe the subensembles of QDs with different sizes. As a result, we observe change in excited level separation: the higher the ground state transition energy, the higher the difference between excited and ground state transitions (Fig. 3), which confirms our interpretation of these PLE spectra in terms of electronic structure. Such size-selective PLE shows 12 to 19 meV energy shift of excited state transitions relative to the ground state transition, while the latter changes by 75 meV. Separation into electron and hole states indicates a change of  $\approx 13$  meV in electron states separation for a 75 meV change in the ground state transition, while the hole states have much lower corresponding change of  $\approx 2$  meV. This extracted size-dependence indicates that level separation energy changes much slower than level localization energy with the change in QD size.

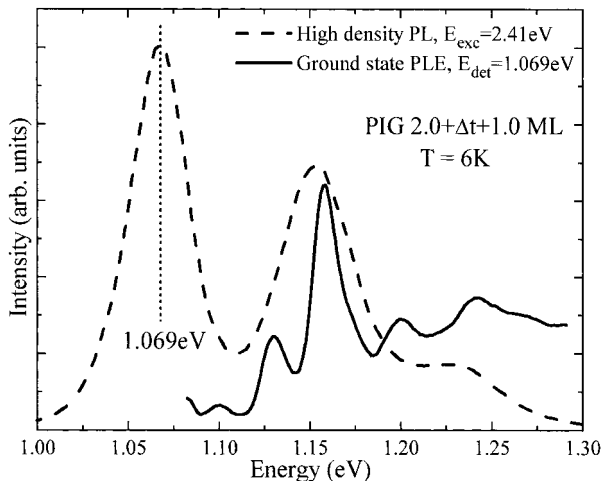


Fig. 2. PLE and high density PL spectra of PIG 2.0 +  $\Delta t$  + 1.0 ML sample

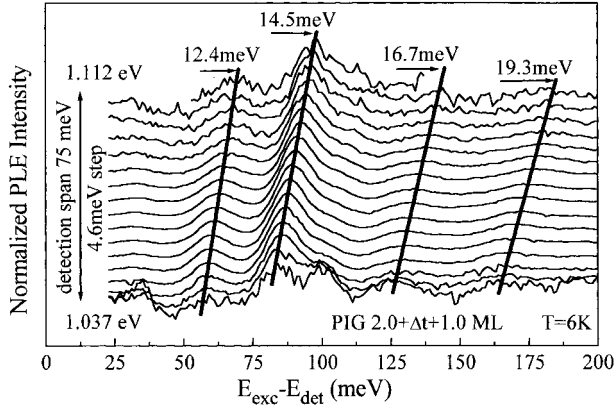


Fig. 3. Size-selective PLE of PIG  $2.0 + \Delta t + 1.0$  ML sample. Spectra are vertically offset for clarity

Inter-band transition signatures are also detected in analogous PIG QD samples grown in  $n$ - $i$ (MQD)- $n$  geometry to allow inter-band and intra-band PC spectroscopy in the FTIR configuration with an integrated cryostat [8]. Details of the structure will be reported elsewhere [9], but it is important to note that the QD region is undoped, and for level population we rely on electron transfer from the  $n$ -doped contact layers. Figure 4 shows a typical normal-incidence room-temperature near-infrared (NIR) PC response, with detected transitions at 0.98, 1.06, 1.14, 1.21 eV, consistent with PL peaks. Typically, NIR PC peaks are much less resolved at LHe temperatures due to decreased probability of carrier extraction and thus suppressed photocurrent. Due to the integrative nature of photocurrent detection, as opposed to the subensemble selection in PLE, one resolves only the strongest transitions in the presence of inhomogeneous broadening. However, intra-band transitions give much richer information on electronic structure since, as found in size-selective PLE, level separations within electron or hole manifolds change much slower than the level energies with change in size. Thus one gets significantly better resolution in the intra-band transitions while inter-band transitions are typically much broader (larger than  $\approx 25$  meV). Figure 5 shows the low tem-

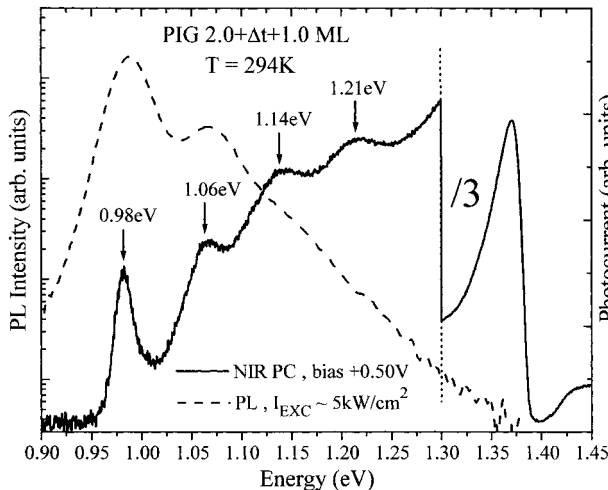


Fig. 4. High density PL and normal-incidence NIR PC spectra of PIG  $2.0 + \Delta t + 1.0$  ML samples. Peaks reflect inter-band transitions

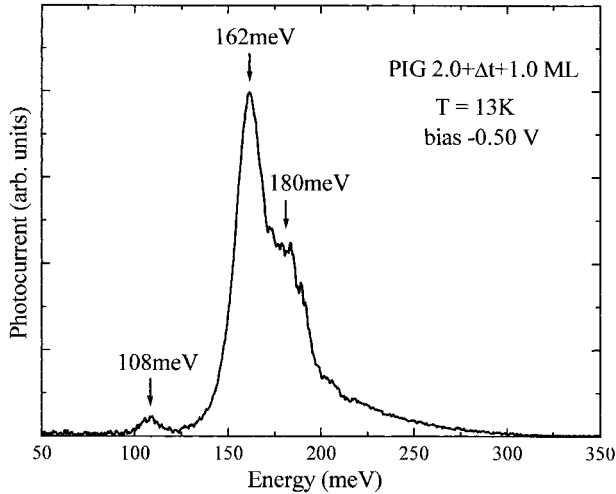


Fig. 5. Normal-incidence MIR PC spectrum of PIG 2.0 +  $\Delta t$  + 1.0 ML sample. Peaks reflect intra-band transitions

perature normal-incidence middle-infrared (MIR) PC intra-band spectrum in the electronic manifold, with two clear peaks at 108 and 162 meV attributed to intra-band bound-to-bound transitions originated from the electron ground state [9]. There is a shoulder indicative of a third peak at  $\approx 180$  meV. However, at present we are not clear about its origin due to its poor reproducibility from sample to sample. According to multipeak fit to PLE data and to calculations available in the literature, one would expect much richer level structure than the two detected peaks. However, one should bear in mind that other possible transitions might be not observed due to small oscillator strengths or due to the depth of the involved level localization. Combining PL/PLE/PC spectroscopies allows us to identify electronic structure as having conduction band states at  $\approx 62$ ,  $\approx 106$ , and  $\approx 162$  meV above the ground state, and valence band states at  $\approx 27$  and  $\approx 67$  meV above the ground state. This, along with QD shape and size derived from AFM/TEM structural characterization, provides a bedframe for testing theoretical models and calculation algorithms.

The temperature dependence of the PL intensity (not shown) indicates two competing nonradiative channels, with activation energies of  $110 \pm 10$  and  $430 \pm 15$  meV. The latter is consistent with QD exciton localization relative to the GaAs bandgap, and the former is attributed to losing nonradiatively one of the carriers (most probably hole) into the wetting layer (WL) state. Such assignment puts a qualitative value of  $150 \pm 50$  meV localization energy for the QD hole ground state, and  $300 \pm 50$  meV localization energy for the QD electron ground state, with respect to the GaAs bands. Electron localization energy correlates with the observation of a weak shoulder in the MIR PC spectra (Fig. 5) extending to  $\approx 300$  meV, implying that for QDs bound-to-continuum transitions are much less efficient than bound-to-bound transitions. Further work is under way to clarify the exact nature of the MIR response.

In conclusion, innovative growth approaches allow us to achieve routinely  $\approx 25$  meV PL linewidth uniform InAs/GaAs QD structures suitable for spectroscopy of QD electronic structure. Structural characterization using AFM and TEM reveals a self-limiting mechanism in QD growth, governed by reduced adatom incorporation probability at highly strained edges once the island becomes large enough, with an estimate of

$\approx 21$  nm on the self-limiting base-size. Large QDs with luminescence at  $\approx 1.07$  eV have  $\approx 0.4$  aspect ratio suggestive of  $\{101\}$  type sidefacets, with typical heights 8 to 9 nm. Complementary PL, PLE, and NIR to MIR PC spectroscopies allow us to identify electronic structure for large islands as having conduction band states at  $\approx 62$ ,  $\approx 106$  and  $\approx 162$  meV above the electron ground state, and valence band states at  $\approx 27$  and  $\approx 67$  meV above the hole ground state. Localization energies are  $300 \pm 50$  and  $150 \pm 50$  meV for electron and hole ground states, relative to GaAs bands. Size-selective PLE shows 12 to 19 meV energy shift of excited state transitions relative to the ground state transition, while the latter changes by 75 meV. Extracted electronic structure and strength of optical transitions qualitatively agree with eight-band  $\mathbf{k} \cdot \mathbf{p}$  calculations reported in Heitz et al. [7] for similar size and shape QDs. The uniformity and narrow PL linewidth of such QD structures have also allowed determination of QD exciton–phonon coupling strength from phonon replica emission [10].

This work was suggested by the US Airforce office of Scientific Research under the MURI program on Nanoscience.

## References

- [1] D. BIMBERG, M. GRUNDMANN, and N. N. LEDENTSOV, *Quantum Dot Heterostructures*, Wiley, Chichester 1999.
- [2] Q. XIE, P. CHEN, A. KALBURGE, T. R. RAMACHANDRAN, A. NAYFONOV, A. KONKAR, and A. MADHUKAR, *J. Crystal Growth* **150**, 357 (1995).
- [3] T. R. RAMACHANDRAN, R. HEITZ, N. P. KOBAYASHI, A. KALBURGE, W. YU, P. CHEN, and A. MADHUKAR, *J. Crystal Growth* **175/176**, 216 (1997).
- [4] I. MUKHAMETZHANOV, Z. WEI, R. HEITZ, and A. MADHUKAR, *Appl. Phys. Lett.* **75**, 85 (1999).
- [5] D. L. HUFFAKER, G. PARK, Z. ZOU, O. B. SHCCKEKIN, and D. G. DEPPE, *Appl. Phys. Lett.* **73**, 2564 (1998).
- [6] G. MEDEIROS-RIBEIRO, A. M. BRATKOVSKI, T. I. KAMINS, D. A. A. OHLBERG, and R. S. WILLIAMS, *Science* **279**, 353 (1998).
- [7] R. HEITZ, O. STIER, I. MUKHAMETZHANOV, A. MADHUKAR, and D. BIMBERG, *Phys. Rev. B*, submitted.
- [8] Z. H. CHEN, O. BAKLENOV, E. T. KIM, I. MUKHAMETZHANOV, A. MADHUKAR, Z. YE, F. MA, B. YANG, and J. CAMPBELL, *QWIP 2000 Workshop*, Dana Point (California), July 2000.
- [9] Z. H. CHEN et al., *J. Appl. Phys.*, in print.
- [10] R. HEITZ, I. MUKHAMETZHANOV, O. STIER, A. MADHUKAR, and D. BIMBERG, *Phys. Rev. Lett.* **83**, 4654 (1999).